Cavity opto-mechanics using an optically levitated nanosphere

D. E. Chang[a], C. A. Regal[b], S. B. Papp[b], D. J. Wilson[b], J. Ye[b,c], O. Painter[d], H. J. Kimble[b,1], and P. Zoller[b,e]

[a]Institute for Quantum Information and Center for the Physics of Information, California Institute of Technology, Pasadena, CA 91125; [b]Norman Bridge Laboratory of Physics 12-33, California Institute of Technology, Pasadena, CA 91125; [c]JILA, National Institute of Standards and Technology, and Department of Physics, University of Colorado, Boulder, CO 80309; [d]Department of Applied Physics, California Institute of Technology, Pasadena, CA 91125; and [e]Institute for Quantum Optics and Quantum Information of the Austrian Academy of Sciences, A-6020 Innsbruck, Austria

Recently, remarkable advances have been made in coupling a number of high-Q modes of nano-mechanical systems to high-finesse optical cavities, with the goal of reaching regimes in which quantum behavior can be observed and leveraged toward new applications. To reach this regime, the coupling between these systems and their thermal environments must be minimized. Here we propose a novel approach to this problem, in which optically levitating a nano-mechanical system can greatly reduce its thermal contact, while simultaneously eliminating dissipation arising from clamping. Through the long coherence times allowed, this approach potentially opens the door to ground-state cooling and coherent manipulation of a single mesoscopic mechanical system or entanglement generation between spatially separate systems, even in room-temperature environments. As an example, we show that these goals should be achievable when the mechanical mode consists of the center-of-mass motion of a levitated nanosphere.

entanglement | optical levitation | quantum information

One of the most intriguing questions associated with quantum theory is whether effects such as quantum coherence and entanglement can be observed at mesoscopic or macroscopic scales. As a first step toward resolving this question, recently much effort has been directed toward quantum state preparation of high-Q modes of nano- and micro-mechanical oscillators—in particular, cooling such modes to their quantum ground state (1). Reaching a regime in which quantum properties such as entanglement (2) emerge is not only of fundamental interest but could lead to new applications in fields such as ultrasensitive detection (3, 4) and quantum information science (5, 6). To reach this regime, it is critical that the thermalization and decoherence rates of these systems be minimized by reducing the coupling to their thermal reservoirs. Thus far, this has necessitated the use of cryogenic operating environments. From an engineering standpoint, it would also be desirable to reduce the dissipation and thermalization rates of these systems through their clamping and material supports (7), so that these rates might approach their fundamental material limits (8).

Here we propose a unique approach toward this problem, wherein the material supports are completely eliminated by optically levitating (9) a nano-mechanical system inside a Fabry–Perot optical cavity. Indeed, since the pioneering work of Ashkin on optical trapping of dielectric particles (9) (in the classical domain), it has been realized that levitation under good vacuum conditions can lead to extremely low mechanical damping rates (10, 11). We show that such an approach should also facilitate the emergence of quantum behavior even in room-temperature environments, when the particles are of subwavelength scale such that the effects of recoil heating due to scattered photons become small. As a specific example, we show that the center-of-mass (CM) motion of a levitated nanosphere can be optically self-cooled (12–14) to the ground state starting from room temperature. This system constitutes an extreme example of environmental isolation because the CM motion is naturally decoupled from the internal degrees of freedom in addition to being mechanically isolated by levitation. In this case, the decoherence and heating rates are fundamentally limited by the momentum recoil of scattered photons and can be reduced simply by using smaller spheres. The long coherence time allowed by small spheres enables the preparation of more exotic states through *coherent* quantum evolution. Here, we consider in detail two examples. First, we describe a technique to prepare a squeezed motional state, which can subsequently be mapped onto light leaving the cavity using quantum state transfer protocols (15–18). Under realistic conditions, the output light exhibits up to ~15 dB of squeezing relative to vacuum noise levels, potentially making this system a viable alternative to traditional techniques using nonlinear crystals (19, 20). Second, we show that entanglement originally shared between two modes of light (21) can be efficiently transferred onto the motion of two spheres trapped in spatially separate cavities, creating well-known Einstein–Podolsky–Rosen (EPR) correlations (22) between the mechanical systems. Our approach of optical levitation mirrors many successful efforts to cool (23, 24), manipulate (25) and entangle (26) the motion of atoms and ions in room-temperature environments. At the same time, our system has a number of potential advantages, in that it enables direct imaging via strong fluorescence, exhibits large trap depths, and has a relatively large mass. We also note recent related experiments involving opto-mechanical "fluids" (with a continuous excitation spectrum rather than discrete modes) in the form of trapped, ultracold atomic gases (27, 28).

Beyond the examples presented here, the use of a levitated device as an opto-mechanical system could provide opportunities on a diverse set of fronts. For instance, it should allow mechanical damping to approach fundamental material limits, potentially enabling the exploration of nanoscale material properties. By levitating systems with internal vibrational modes, multiple modes could be optically addressed and cooled. In addition, the CM oscillation frequency can be tuned through the trapping intensity, allowing for adiabatic state transfer (29) with other modes or matching spatially separate systems for optical linking and entanglement generation (30). Furthermore, this paradigm integrates nano-mechanics with many techniques for atomic trapping and manipulation, which can be further extended by levitating systems containing an internal electronic transition (e.g., a color center within a nano-crystal) (31). Finally, as illustrated by squeezed light generation, engineering mechanical nonlinearities in conjunction with quantum state transfer yields a unique means to realize nonlinear optical processes.

PHYSICS

Optical Forces and Noise Acting on a Dielectric Sphere

To illustrate our idea, we consider a subwavelength dielectric sphere interacting with two standing-wave optical modes of a Fabry–Perot cavity (Fig. 1A). One resonantly driven mode provides an optical dipole trap for the sphere. The second mode is driven by a weaker "cooling" beam, assumed to have a nonzero intensity gradient at the trap center, which provides a radiation pressure cooling force (12–14). We discuss the cooling mechanism in the next section, whereas here we focus on the trapping potential and the noise forces acting on the sphere.

The trapping beam provides a gradient force similar to that used to "optically tweeze" small dielectric particles (9). Considering a sphere whose radius is much smaller than the optical wavelength, $r \ll \lambda$, its optical response is like that of a point dipole with induced dipole moment $p_{ind} = \alpha_{ind} E(x)$ and optical potential $U_{opt}(x) = -(1/4)(\text{Re }\alpha_{ind})|E(x)|^2$ (*SI Text*). Here x is the CM position of the sphere along the cavity axis, $\alpha_{ind} = 3\epsilon_0 V\left(\frac{\epsilon-1}{\epsilon+2}\right)$ is its polarizability, V is the sphere volume, and ϵ is the electric permittivity. Taking a standing wave $E(x) = E_0 \cos kx$ ($k \equiv 2\pi/\lambda$), to lowest order near an antinode the potential corresponds to a harmonic oscillator with mechanical frequency

$$\omega_m = \left(\frac{6k^2 I_0}{\rho c} \text{Re}\frac{\epsilon-1}{\epsilon+2}\right)^{1/2}, \qquad [1]$$

where I_0 is the field intensity and ρ is the mass density of the sphere. The total trap depth is $U_0 = (3I_0 V/c)\text{Re}\frac{\epsilon-1}{\epsilon+2}$. Typical trap depths and oscillation frequencies are plotted in Fig. 1C and D. For all numerical examples, we take material properties $\epsilon = 2$, $\rho = 2$ g/cm³ corresponding to fused silica and an operating wavelength $\lambda = 1$ μm. Frequencies of $\omega_m/2\pi \sim 0.5$ MHz are achievable using an intracavity intensity of $I_0 \sim 0.1$ W/μm². The imaginary component of ϵ characterizes optical absorption, which contributes to an increase ΔT_{int} in the internal temperature of the sphere. Assuming a value corresponding to ~10 dB/km propagation losses in bulk, intensities of $I_0 \sim 10$ W/μm² can be sustained without melting the sphere, due to blackbody reradiation of the absorbed energy (*SI Text*). We believe that this loss value is realistic, given that even lower values around these wavelengths have been observed in fused silica (32).

The dominant noise forces acting on the sphere are collisions with a background gas and momentum recoil kicks due to scattered photons. In *SI Text*, we show that the contributions from shot noise, blackbody radiation, and sphere anisotropy are negligible. Furthermore, the CM is decoupled from the internal degrees of freedom and the sphere effectively has no internal structure (as opposed to molecules, where the internal configuration can affect cooling efficiency) (33). In the regime in which the molecular mean free path exceeds r, the background gas leads to a mean damping force $dp/dt = -\gamma_g p/2$ with damping rate $\gamma_g/2 = (8/\pi)(P/vr\rho)$, where P and v are the background gas pressure and mean speed, respectively (34). The random nature of the collisions also thermalizes the motional energy at a rate given through the fluctuation–dissipation theorem by $dE/dt = -\gamma_g(E - k_B T)$, where T is the gas temperature. In particular, the characteristic time for the system to heat by one phonon starting from the ground state is $\tau_g = \hbar\omega_m/\gamma_g k_B T$. Note that τ_g^{-1} does not necessarily reflect the actual collision rate between the sphere and gas molecules, $R_{coll} \approx \pi P v r^2/k_B T$ (it is possible for a single collision to be quite rare, $R_{coll} \ll \tau_g^{-1}$, and to impart several phonons at once). We define a mechanical quality factor $Q_g = \omega_m/\gamma_g$ due to the background gas and a number of coherent oscillations $N_{osc}^{(g)} \equiv \omega_m \tau_g/2\pi$ expected before the energy increases by a single phonon. For a sphere of radius $r = 50$ nm, $\omega_m/2\pi = 0.5$ MHz, and a room-temperature gas with $P = 10^{-10}$ Torr, one finds $\gamma_g \sim 10^{-6}$ s⁻¹, $Q_g \sim 3 \times 10^{12}$, $N_{osc}^{(g)} \sim 4 \times 10^4$, indicating that an ideal nanosphere can be essentially decoupled from its thermal environment.

Photons scattered by the sphere out of the cavity lead to heating and decoherence of the motion. In particular, a scattering event entangles the mechanical and photonic wave functions because the phase of the outgoing photon becomes correlated with the position of the scatterer. Tracing out the photonic degrees of freedom, the density matrix $\hat{\rho}$ describing the motion evolves after
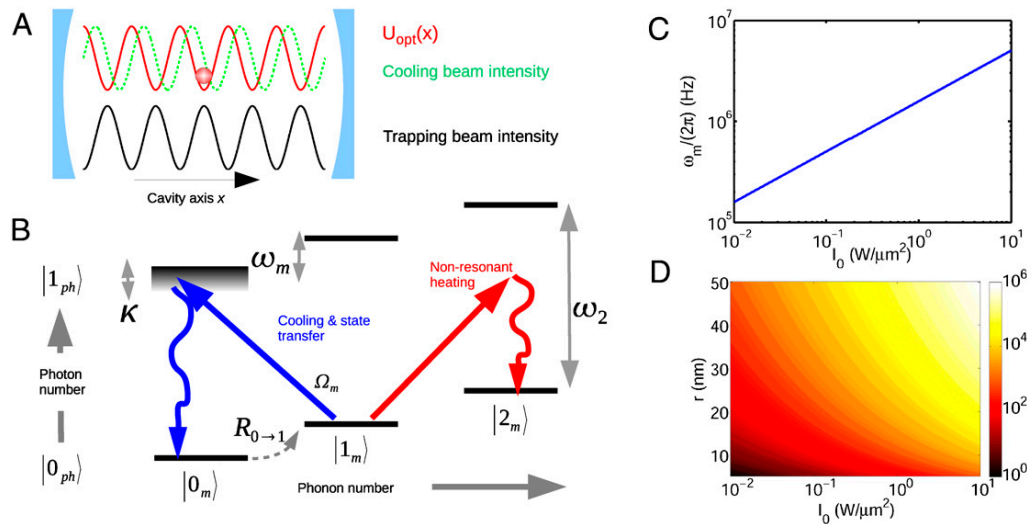

Figure 1. A) Illustration of dielectric sphere trapped in optical cavity. The large trapping beam intensity provides an optical potential $U_{opt}(x)$ that traps the sphere near an antinode. A second more weakly driven cavity mode with a nonvanishing intensity gradient at the trap center is used to cool the motion of the sphere. B) Energy level diagram of mechanical motion (denoted m) and cavity cooling mode (ph). The mechanical mode has frequency ω_m, while the optical mode has frequency ω_2 and linewidth κ. Photon recoil induces transitions between mechanical states $|n_m\rangle \rightarrow |(n \pm 1)_m\rangle$ at a rate $R_{n \rightarrow n \pm 1}$ ($R_{0 \rightarrow 1}$ shown by dashed gray arrow). The cooling beam, with effective optomechanical driving amplitude Ω_m, induces anti-Stokes scattering that cools the mechanical motion and allows for quantum state transfer between motion and light. This beam is also responsible for weaker, off-resonant heating via Stokes scattering. C) Mechanical frequency ω_m as a function of trapping beam intensity. For all numerical results, we take $\lambda = 1$ μm, $\rho = 2$ g/cm³, and $\epsilon = 2$. D) Optical trap depth U_0 (in K) as functions of trapping beam intensity and sphere radius r.

Chang et al.

a scattering event as $\hat{\rho} \rightarrow \int d\mathbf{k} P(\mathbf{k}) e^{i\mathbf{k}\cdot\hat{\mathbf{r}}} \hat{\rho} e^{-i\mathbf{k}\cdot\hat{\mathbf{r}}}$ (35). Here $P(\mathbf{k})$ is the probability distribution of the scattered photon wavevector, and $\hat{\mathbf{r}}$ is the CM position operator. In analogy with atoms or ions trapped in the Lamb–Dicke regime (25), when the particle is trapped on a scale $\Delta x \ll 1/k$, the terms $e^{\pm i\mathbf{k}\cdot\hat{\mathbf{r}}}$ can be expanded to first order in $\mathbf{k}$. This describes transitions between consecutive harmonic oscillator levels $n \rightarrow n \pm 1$, with rates $R_{n\rightarrow n\pm 1} = \gamma_{sc}(n + 1/2 \pm 1/2)$. Considering motion only along the x direction,

$$\gamma_{sc} = (2/5)(\omega_r/\omega_m)R_{sc} \qquad [2]$$

where $\omega_r = \hbar k^2/2\rho V$ is the recoil frequency and R_{sc} is the photon scattering rate. A result identical to Eq. **2** holds for a weakly excited, trapped atom (36). In the case of the sphere, $R_{sc} = 48\pi^3 \frac{I_0 V^2}{\lambda^4 \hbar \omega} (\frac{\epsilon-1}{\epsilon-2})^2$, as can be obtained by taking the power radiated by a dipole of strength p_{ind} and dividing by the energy $\hbar\omega$ per photon. We emphasize that in the Lamb–Dicke regime, the effect of photon scattering on motional heating and decoherence is completely described by Eq. **2**. On the other hand, the above transformation of the density matrix $\hat{\rho}$ is completely general. For example, when the motional wave packet has a spatial extent $\Delta x \sim \lambda$, one finds then that a single scattering event can destroy quantum coherence (37). Analogous effects also occur due to absorption and emission of blackbody photons. In our system, however, such effects are negligible because $\Delta x \ll 1/k$ (i.e., $\omega_r/\omega_m \ll 1$ in Eq. **2**), and the emission rate of blackbody photons is much smaller than R_{sc}.

It is convenient to define a dimensionless parameter

$$\phi \equiv \gamma_{sc}/\omega_m = \frac{4\pi^2}{5} \frac{\epsilon-1}{\epsilon+2} (V/\lambda^3) \qquad [3]$$

to characterize the strength of photon recoil heating, which primarily depends on the sphere volume compared to the cubic wavelength. This scaling reflects the fact that the scattered power and dipole force scale like p_{ind}^2 and p_{ind}, respectively. We emphasize that the effect of recoil heating can be reduced by simply using smaller spheres. In the limit that optical scattering is the dominant heating process, the expected number of coherent oscillations is $N_{osc}^{(sc)} = 1/(2\pi\phi) \propto \lambda^3/V$. We will find that ϕ naturally appears to characterize the fundamental limits to observing quantum behavior in our system. For a sphere of radius $r = 50$ nm, $\epsilon = 2$, and $\lambda = 1$ μm, one finds that $N_{osc}^{(sc)} \sim 150$. Comparing with background gas collisions at $P = 10^{-10}$ Torr and $\omega_m/2\pi = 0.5$ MHz, recoil heating dominates N_{osc} for sphere sizes $r \gtrsim 10$ nm. Reaching the regime $N_{osc} \gg 1$ implies that the sphere can coherently evolve for many oscillation periods after any cooling mechanisms are turned off, which makes this system a promising candidate for observing coherent quantum phenomena.

Finally, we remark that R_{sc} can be very large ($R_{sc} \sim 10^{14}$ s^{-1} for $I_0 = 1$ W/μm^2 and $r = 50$ nm) compared to atoms or ions, which enables direct imaging. The large scattering is due to the large intensities and the linear response of the sphere (it does not saturate like an atom or ion), as opposed to the system behaving as a lossy element in the cavity. The contribution to the cavity loss rate is $\kappa_{sc} = 12\pi^2\omega(V^2/\lambda^3 V_c)(\frac{\epsilon-1}{\epsilon+2})^2$, where V_c is the cavity mode volume, and κ_{sc} is typically much smaller than the natural cavity linewidth κ.

Cooling the Center-of-Mass Motion to the Ground State

We now describe the optical cooling effect of the weaker, second cavity mode (denoted mode 2). For concreteness, we assume that the sphere is trapped near the antinode $x = 0$ of cavity mode $E_1 \propto \cos k_1 x$ and that the second mode has spatial profile $E_2 \propto \cos(k_2 x - \pi/4)$ such that the intensity gradient is maximized. The total Hamiltonian of the system is given in a rotating frame by

$$H = -\hbar\delta_1 \hat{a}_1^\dagger \hat{a}_1 - \hbar g_1(\cos 2k_1\hat{x} - 1)\hat{a}_1^\dagger \hat{a}_1 - \hbar\delta_2 \hat{a}_2^\dagger \hat{a}_2$$
$$- \hbar g_2 \cos 2(k_2\hat{x} - \pi/4)\hat{a}_2^\dagger \hat{a}_2 + \frac{\hat{p}^2}{2m}$$
$$+ \frac{\hbar\Omega}{2}[(\hat{a}_1 + \hat{a}_1^\dagger) + \sqrt{2\zeta'}(\hat{a}_2 + \hat{a}_2^\dagger)]. \qquad [4]$$

Here $\hat{p}$ and $\hat{x}$ are the momentum and position operators of the CM, $\hat{a}_i$ is the photon annihilation operator of cavity mode i, and Ω and $\Omega\sqrt{2\zeta'}$ are the driving amplitudes of modes 1 and 2, respectively. δ_i is the detuning between the driving field and mode frequency when the sphere sits at $x = 0$. The opto-mechanical coupling strengths $g_i = \frac{3V}{4V_{c,i}}\frac{\epsilon-1}{\epsilon+2}\omega_i$ characterize the position-dependent frequency shifts due to the sphere (*SI Text*), where $V_{c,i}$ and ω_i are the mode volume and resonance frequency of mode i. To simplify notation, we assume that modes 1 and 2 have similar properties, $\omega_1 \approx \omega_2 = \omega$, etc. In addition to the evolution described by H, the system also exhibits cavity losses and the mechanical noise described previously.

Expanding the opto-mechanical coupling term of mode 2 around $x = 0$, $\hbar g\cos 2(k\hat{x} - \pi/4)\hat{a}_2^\dagger \hat{a}_2 \approx 2\hbar gk\hat{x}\hat{a}_2^\dagger \hat{a}_2$, one finds a linear coupling in the sphere position analogous to the effect of radiation pressure on a moving mirror of a Fabry–Perot cavity (13). Physically, the motion induces changes in the detuning and thus the intracavity field amplitude, while the lag in the cavity response enables the field to do work (cooling) on the sphere. Following the techniques of ref. 13, to calculate the cooling rate we first apply shifts to the operators, $\hat{a}_i \rightarrow \hat{a}_i + \alpha_i$ and $\hat{x} \rightarrow \hat{x} + x_0$, where α_i and $x_0 \approx \zeta/k$ [$\zeta \approx \kappa^2\zeta'/(\kappa^2 + 4\delta_2^2)$] are mean values of the quantum fields. Here we have defined $2\zeta = |\alpha_2/\alpha_1|^2$ as the ratio of intracavity intensities of modes 1 and 2 and assumed that mode 1 is driven on resonance ($\delta_1 = 0$). To lowest order in ζ, field mode 1 (mode 2) is purely responsible for trapping (cooling). Subsequently tracing out the cavity degrees of freedom yields equations for the mechanical motion alone. In particular, to lowest order in ζ and for $\delta_2 < 0$, the cooling laser provides a net cooling rate $\Gamma \equiv R_{opt,-} - R_{opt,+} = \kappa\Omega_m^2[((\delta_2 + \omega_m)^2 + (\kappa/2)^2)^{-1} - ((\delta_2 - \omega_m)^2 + (\kappa/2)^2)^{-1}]$ (*SI Text*), where $R_{opt,\mp}$ denote the anti-Stokes (cooling) and Stokes (heating) scattering rates (see Fig. 1B). Here $\Omega_m \equiv 2gkx_m|\alpha_1|\sqrt{2\zeta}$ is the effective opto-mechanical driving amplitude (see Fig. 1B) and $x_m \equiv \sqrt{\hbar/2m\omega_m}$. Validity of these perturbative results requires $\Omega_m \lesssim \kappa, \omega_m$ and $\zeta \lesssim 1$.

In the realistic limit that background gas collisions are negligible, the steady-state phonon number is $\langle n_f \rangle \approx \tilde{n}_f + \gamma_{sc}/\Gamma$, where $\tilde{n}_f = R_{opt,+}/\Gamma$ is the fundamental limit of laser cooling (13). It is minimized when $\delta_2 = -(1/2)\sqrt{\kappa^2 + 4\omega_m^2}$. In particular, when sideband resolution is achieved ($\omega_m \gtrsim \kappa$), $\tilde{n}_{f,min} \approx (\kappa/4\omega_m)^2 \ll 1$, indicating that ground-state cooling is possible provided other heating mechanisms are made sufficiently small. Considering the limit $\omega_m \gg \kappa$ and taking the maximum cooling rate $\Gamma \sim \kappa$ consistent with the perturbative calculations, using Eq. **3** one can then rewrite $\langle n_f \rangle$ as

$$\langle n_f \rangle \approx \frac{\kappa^2}{16\omega_m^2} + \phi\frac{\omega_m}{\kappa}. \quad (\omega_m \gg \kappa) \qquad [5]$$

The last term on the right corresponds to photon recoil heating. Eq. **5** is minimized for $\kappa/\omega_m = 2\phi^{1/3}$, in which case $\langle n_f \rangle_{min} = 3\phi^{2/3}/4 \propto (r/\lambda)^2 \ll 1$. Thus, one sees that ground-state cooling is readily attainable (provided that $\zeta \lesssim 1$ can be simultaneously satisfied). Physically, the optimum value of κ/ω_m balances good sideband resolution and excessive heating when large intensities are used to increase ω_m.

To illustrate these results, we consider a fused silica sphere of radius $r = 50$ nm and $\omega_m/(2\pi) = 0.5$ MHz levitated inside

PHYSICS

a cavity of length $L = 1$ cm and mode waist $w = 25$ μm ($V_c = (\pi/4)Lw^2$). In Fig. 2A we plot the minimum obtainable $\langle n_f \rangle$ (black curve) as a function of cavity finesse $\mathscr{F} \equiv \pi c/\kappa L$, assuming negligible gas collisions and subject to the constraints 2ζ, Ω_m/κ, $\Omega_m/\omega_m < 1/2$ and optimized over detuning δ_2. For low cavity finesse the cooling is nearly limited by sideband resolution ($\tilde{n}_{f,\mathrm{min}}$, red curve), and the ground-state regime $\langle n_f \rangle < 1$ can be reached with a minimum finesse of $\mathscr{F} \sim 10^4$. A minimum of $\langle n_f \rangle \sim 0.01$ is reached at a finesse of $\mathscr{F} \sim 3 \times 10^5$, with a maximum cooling rate of $\Gamma \sim \kappa \sim 3 \times 10^5$ s^{-1} (see Table 1 for a summary of parameters). This corresponds to a final temperature of $T_f \sim 5$ μK, or a remarkable compression factor of $T/T_f \sim 6 \times 10^7$ relative to room temperature T. We note that values of $\mathscr{F} \sim 10^6$ have been achieved in Fabry–Perot cavities at similar wavelengths (38).

Thus far, we have only considered the motion along the cavity axis. With additional cavities oriented along different axes, clearly it is possible to achieve 3D ground-state cooling of the CM motion. Moreover, due to the high rate of Rayleigh scattering, feedback cooling can be readily applied for transverse localization. However, as shown in *SI Text*, the transverse motion need not be reduced below the level set by the ambient environment. Specifically, one only requires that the transverse position uncertainty Δy be small compared to the beam waist w, as the transverse motion introduces errors of order $(\Delta y/w)^2$ (e.g., in the fractional decrease in cooling efficiency). For the parameters of Table 1, thermal motion at $T = 300$ K yields only $(\Delta y/w)^2 \sim 10^{-2}$ due to the large trap depth, while recoil heating leads to a position uncertainty $\Delta y/w \approx \sqrt{\phi \omega_r t}$ in the absence of any transverse cooling mechanism. Note that result of recoil heating is intensity-independent, since an increase in intensity leads to equal increases in the photon scattering rate and the transverse confinement of the optical potential. One finds that recoil heating is a very weak effect, as a time $t \sim 5{,}000$ s is required to reach the regime $(\Delta y/w)^2 \sim 10^{-2}$.

Motional Entanglement and Squeezed Light Generation Using Quantum State Transfer

A number of related schemes have been proposed for quantum state transfer between light and the motion of atoms (15, 16) or nano-mechanical systems (17, 18). In our system, the small mechanical noise and ease of achieving good sideband resolution in principle allow state transfer to be realized with almost perfect efficiency. This might enable light with nonclassical properties to be mapped onto mechanical motion (39), and as an example, we show that this can be used to generate EPR correlations between two spatially separate spheres. Moreover, a complementary process can be realized, where a nontrivial mechanical state (a squeezed state) is prepared through coherent manipulation and subsequently transferred to light leaving the cavity. The latter case illustrates how opto-mechanics can yield a novel nonlinear optical system.

First we give a simplified picture of quantum state transfer using a one-sided, ideal cavity (where all losses are via transmission through one cavity mirror) (40). Specifically, we consider the Heisenberg equations of motion in a rotating frame for the cavity cooling mode and the motion (after applying the shifts described in the previous section), when the cooling mode is driven resonantly on the red motional sideband ($\delta_2 = -\omega_m$),

$$\frac{d\hat{a}_2}{dt} = -\frac{\kappa}{2}\hat{a}_2 - i\Omega_m(\hat{b} + \hat{b}^\dagger e^{2i\omega_m t}) + \sqrt{\kappa}\hat{a}_{2,\mathrm{in}},$$

$$\frac{d\hat{b}}{dt} = (i/\hbar)[H_e, \hat{b}] - i\Omega_m(\hat{a}_2 + \hat{a}_2^\dagger e^{2i\omega_m t}) + i\hat{F}(t)e^{i\omega_m t}. \quad [6]$$

The Hamiltonian H_e describes any external forces or couplings applied to the sphere beyond those in Eq. **4**, $\hat{b}$ is the annihilation operator corresponding to a harmonic oscillator of mass m and frequency ω_m, and $\hat{a}_{2,\mathrm{in}}$ is the cavity input operator associated with losses. $F(t)$ is the (Hermitian) noise due to photon recoil, which has correlations $\langle F(t)F(t') \rangle = \phi \omega_m \delta(t - t')$, and we assume all other noise is negligible. Since the cavity trapping mode ($\hat{a}_1$) effectively provides a harmonic potential and can otherwise be ignored, for simplicity we will omit the subscript 2 as we refer to the cooling mode in future discussions. Temporarily assuming that the nonsecular terms ($e^{2i\omega_m t}$) can be ignored and that the mechanical motion evolves slowly on time scales compared to $1/\kappa$, one can adiabatically eliminate the cavity mode to yield $\hat{a} \approx -2i(\Omega_m/\kappa)\hat{b} + (2/\sqrt{\kappa})\hat{a}_{\mathrm{in}}$, and $d\hat{b}/dt \approx (i/\hbar)[H_e, \hat{b}] - (\Gamma/2)\hat{b} - i\sqrt{\Gamma}\hat{a}_{\mathrm{in}} + i\hat{F}(t)e^{i\omega_m t}$, where $\Gamma \equiv 4\Omega_m^2/\kappa$ is the cavity-induced cooling rate in the weak-driving limit ($\Omega_m \lesssim \kappa$). The cavity output is related to the input and intracavity fields through $\hat{a}_{\mathrm{out}} = \sqrt{\kappa}\hat{a} - \hat{a}_{\mathrm{in}}$ (40), or $\hat{a}_{\mathrm{out}} \approx -i\sqrt{\Gamma}\hat{b} + \hat{a}_{\mathrm{in}}$, which states that the mechanical motion is mapped onto the outgoing light. Physically, the cooling process converts phononic excitations into photonic excitations that leak out of the cavity. Generally, two mechanisms will degrade state transfer. First, $\hat{F}$ adds extra noise to the ideal state that one is attempting to transfer, with a strength characterized by the small parameter ϕ. Second, the nonsecular terms contribute to Stokes scattering, destroying the perfect phonon-photon correspondence, with a strength that is expected to be proportional to $(\kappa/\omega_m)^2$. Given that ϕ, $(\kappa/\omega_m)^2$ can be made small, nearly perfect state transfer is possible in principle. We illustrate this with two examples, entanglement transfer and squeezed light generation.

Entanglement Transfer. Here we describe how EPR correlations shared between two modes of light (21) can be mapped to the motion of two spheres trapped in spatially separate cavities. Specifically, we define quadrature operators for the input light for each of the two systems (denoted A, B), given by $X_{+,\mathrm{in}}^{(j)} =$
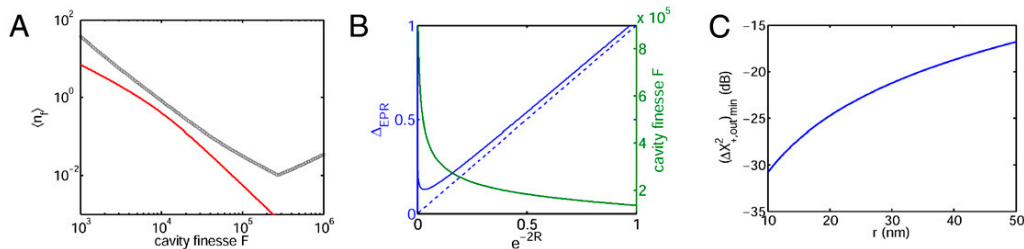

Figure 2. A) Mean phonon number $\langle n_f \rangle$ (black curve) versus cavity finesse $\mathscr{F}$ ($\mathscr{F} = \pi c/\kappa L$) under optimized cooling conditions. The system parameters are given in Table 1. The red curve denotes $\tilde{n}_{f,\mathrm{min}}$, the fundamental limit of cooling imposed by sideband resolution. B) Solid blue curve: optimized EPR variance between two levitated spheres, as a function of squeezing parameter e^{-2R}. System parameters are identical to a). Dashed curve: EPR variance in limit of perfect state transfer, $\Delta_{\mathrm{EPR}} = e^{-2R}$. Green curve: cavity finesse corresponding to optimal EPR variance. C) Optimized variance $(\Delta X_{+,\mathrm{out}}^2)_{\mathrm{min}}$ (in dB) of squeezed output light from an ideal cavity, as a function of sphere size.

Chang et al.

Table 1. Example cooling parameters for a fused silica sphere of radius $r = 50$ nm at $\lambda = 1\ \mu m$

Cavity length	Beam waist	Cavity finesse $\mathscr{F}$	Total cavity decay $\kappa/2\pi$, scattering contribution $\kappa_{sc}/2\pi$	Mechanical frequency $\omega_m/2\pi$	Intracavity intensities: trapping, cooling beams	Internal heating ΔT_{int}	Photon scattering rate R_{sc} (both beams)	Phonon number $\langle n_f \rangle$
1 cm	25 μm	3×10^5	5×10^4, 100 Hz	0.5 MHz	0.1, 0.05 W/μm^2	80 K	1.6×10^{13} s^{-1}	0.01

$(\hat{a}_{in}^{(j)} + \hat{a}_{in}^{(j)\dagger})$, $X_{-,in}^{(j)} = (\hat{a}_{in}^{(j)} - \hat{a}_{in}^{(j)\dagger})/i$ for $j = A, B$. A similar set of operators $X_{\pm,m}^{(j)}$, $X_{\pm,out}^{(j)}$ can be defined for the motion and output light, by replacing $\hat{a}_{in}^{(j)} \to \hat{b}^{(j)}$, $\hat{a}_{out}^{(j)}$, respectively. Of particular interest is the case where the two input fields exhibit broadband EPR correlations between them,

$$\langle (X_{\pm,in}^{(A)}(\omega) \pm X_{\pm,in}^{(B)}(\omega))^2 \rangle/2 = e^{-2R} < 1. \quad [7]$$

When the variances satisfy $e^{-2R} < 1$, the two modes exhibit correlations below vacuum level and are entangled (41) (for concreteness, we assume the other combinations of quadratures satisfy $\langle (X_{\pm,in}^{(A)}(\omega) \mp X_{\pm,in}^{(B)}(\omega))^2 \rangle/2 = e^{2R}$). Such EPR correlations have been observed with light and in the internal degrees of freedom of atomic ensembles (42), but have yet to be demonstrated using mechanical systems.

To proceed, we solve Eq. **6** in the Fourier domain (including the nonsecular terms) for each of the systems for the correlations given in Eq. **7** and $H_e = 0$. Generally, the nonsecular terms yield an infinite set of algebraic equations (coupling frequencies $\omega_m + 2n\omega_m$ for integer n), which given $\omega_m \gg \Omega_m, \kappa$ can be truncated to good approximation at $n > 1$. For simplicity of analysis, we assume the two systems have identical properties, and that the cooling rate $\Gamma = \kappa$. However, we expect our results should qualitatively hold provided that only Γ, ω_m of the two systems are properly tuned, which can be easily accomplished by adjusting the trapping and cooling beam intensities. One can then show that state transfer yields the following joint variances in the motion (*SI Text*),

$$\Delta_{EPR} \equiv \langle (X_{\pm,m}^{(A)}(t) \mp X_{\pm,m}^{(B)}(t))^2 \rangle/2$$
$$= e^{-2R} + \frac{\kappa^2}{16\omega_m^2}(3e^{2R} + 2\sinh 2R) + \frac{4\phi\omega_m}{\kappa}. \quad [8]$$

As expected, Stokes scattering and recoil heating contribute to the variance by amounts $(\kappa/\omega_m)^2$ and $\phi\omega_m/\kappa$, respectively. This can be minimized with respect to κ/ω_m, yielding $\Delta_{EPR,min} = e^{-2R} + 3(\phi/2)^{2/3}(3e^{2R} + 2\sinh 2R)^{1/3}$. To illustrate these results we plot $\Delta_{EPR,min}$ in Fig. 2B as a function of e^{-2R}, taking the same parameters as in Fig. 2A. For the moderate values of e^{-2R} typically obtained in experiments (21), EPR correlations in the motion can be achieved with reasonable cavity finesse $\mathscr{F} \sim 10^5$.

Squeezed Light Generation. First we describe a technique to create a mechanical squeezed state and then derive the properties of the outgoing light upon quantum state transfer. Mechanical squeezing is accomplished by adding a sinusoidally varying component to the intensity of the trapping beam, which yields the Hamiltonian of a parametric amplifier (43), $H_e = \epsilon_m \omega_m^2 x^2 \sin 2\omega_m t$. Here ϵ_m is a small parameter characterizing the strength of the modulation of the trap frequency. As one approaches the threshold for parametric oscillation ($\epsilon_m \omega_m \to \Gamma$), the variance in one quadrature of motion is reduced by up to a factor of 2 (43).

We now investigate the properties of the outgoing light over a narrow frequency range near the cavity resonance, specifically considering $X_{\pm,out}(\omega = 0)$. We apply similar methods as above to solve Eq. **6** in the Fourier domain. Taking the limit as one approaches threshold and $\Gamma = \kappa$, the variance in the output light is given by (*SI Text*)

$$\Delta X_{+,out}^2(\omega = 0) = \frac{2\phi\omega_m}{\kappa} + \frac{5}{16}\frac{\kappa^2}{\omega_m^2}. \quad [9]$$

Again, an optimum value of $\kappa/\omega_m \propto \phi^{1/3}$ maximizes the squeezing, with a minimum variance of $(\Delta X_{+,out}^2)_{min} \approx 2.04\phi^{2/3}$. Thus for small sphere sizes the noise level can be reduced far below that of the vacuum state (corresponding to $\Delta X_{+,out}^2 = 1$). A plot of $(\Delta X_{+,out}^2)_{min}$ as a function of sphere size is shown in Fig. 2C. For $r = 10$ nm size spheres, one finds that $\sim$30 dB of noise reduction relative to the vacuum state can be obtained using an ideal cavity (note that for a background gas pressure of $P \sim 10^{-10}$ Torr, additional noise arising from gas collisions is negligible down to $r \sim 10$ nm).

In practice, a cavity has additional scattering and absorption losses that limit the squeezing. Starting from Eq. **9**, which gives the amount of squeezing at threshold using an ideal cavity (with $\Gamma = \kappa$), we model cavity losses via a beam splitter transformation with the ideal squeezed light and vacuum as the two inputs. The output light exhibits reduced squeezing due to mixing with the vacuum, given by

$$(\Delta X_{+,out}^2(\omega = 0))_{min} = \left(1 - \frac{\kappa'}{\kappa}\right)\left(\frac{2\phi\omega_m}{\kappa} + \frac{5}{16}\frac{\kappa^2}{\omega_m^2}\right) + \frac{\kappa'}{\kappa}, \quad [10]$$

where κ', κ denote the scattering/absorption loss in the cavity and the total cavity linewidth, respectively. In the relevant regime where $\kappa'/\kappa \ll 1$, we can approximate $1 - \kappa'/\kappa \approx 1$ and the squeezing is optimized for the choice $\kappa/\omega_m = 2(2/5)^{1/3}(\phi + \kappa'/(2\omega_m))^{1/3}$, for which $(\Delta X_{+,out}^2)_{min} \approx 2.04(\phi + \kappa'/(2\omega_m))^{2/3}$. We now must choose a set of realistic cavity parameters where this optimized squeezing can be realized, and where $\Gamma = \kappa$ is consistent with ζ being small. As an example, taking a cavity length and waist of $L \sim 2$ cm and $w \sim 10\ \mu m$, κ' corresponding to 1 ppm losses per round trip (38), and sphere parameters $r = 50$ nm and $\omega_m/(2\pi) = 0.5$ MHz, we find that $\Gamma = \kappa$ corresponds to a value $\zeta \sim 1/4$, which yields squeezing of $\sim$15 dB in the output light.

In principle, similar techniques also apply to trapped atoms or ions. However, one benefits from the relatively large mass m of the sphere. Specifically, approaching threshold, one quadrature of motion becomes infinitely unsqueezed, producing a large position uncertainty Δx (43). At the same time, faithful quantum state transfer requires a linear opto-mechanical coupling, which translates into a requirement that the spatial extent Δx of the motional state of the nanosphere be well-localized with respect to the wavelength λ_0 of the trapping laser and the wavelengths λ_s for any incoherent scattering events. Taking $\lambda_0 = \lambda_s = 2\pi/k$ as relevant to the nanosphere, we require that $k\Delta x \approx k\sqrt{\frac{\hbar n}{2m\omega_m}} \ll 1$, where n characterizes the average phonon number. In *SI Text*, we show that $k\Delta x < 10^{-2}$ can be satisfied with a sphere even in the regime of $\sim$30 dB squeezing. To compare, a "typical" atom of mass $m_a = 100$ amu trapped with frequency $\omega_m/(2\pi) = 0.5$ MHz has a ground-state wavepacket of size $x_a \approx 10$ nm, so that $\Delta x \approx x_a n^{1/2} \approx 320$ nm. Hence, a linear coupling cannot be achieved for optically trapped atoms for the requisite n, while

PHYSICS

linear coupling is possible for ion traps. However, in both cases, a single scattered photon would substantially decohere the motional quantum state of the atom, as Δx is comparable to λ_s.

The amount of squeezing predicted in this opto-mechanical system compares favorably with traditional techniques involving a nonlinear optical crystal pumped inside a cavity, where squeezing of ~10 dB has recently been observed (19, 20). An important limitation in these experiments appears to be nonlinear absorption of the crystal (19), which currently prevents significantly greater squeezing even if all other imperfections are eliminated. On the other hand, the mechanical noise in our system in principle enables squeezing by up to ~30 dB, limited only by cavity losses and extraction efficiency. With state-of-the-art Fabry–Perot cavities, we anticipate that up to ~15 dB of squeezing in the output light can be achieved. Even higher levels should be possible by coupling the levitated particle to microsphere cavities to take advantage of their small mode volumes and remarkable quality factors (44), provided that trapping techniques near such structures can be developed.

Outlook

An optically levitated opto-mechanical system can have remarkably long coherence times, which potentially enables quantum phenomena such as entanglement to be observed even in room-temperature environments. Combining previously demonstrated techniques to controllably grow small particles (45) and load and manipulate them in vacuum (9, 46) should put this system within immediate experimental reach. Extending the ideas presented here should open up several other interesting possibilities. First, we anticipate that our techniques to achieve environmental isolation and use optical forces to engineer the mechanical motion are applicable to a large class of opto-mechanical systems beyond dielectric nano-particles. For example, by introducing specifically tailored optical potentials, it should be possible to produce nontrivial dynamics, such as nonlinear motion. In addition, several nano-particles or more complex nano-mechanical systems with internal modes could be levitated and coupled together, for the purpose of entangling multiple degrees of freedom. Finally, by levitating charged or magnetic systems, one could potentially realize systems analogous to ion traps (47) or facilitate novel quantum hybrid architectures (6).

Note added: We have become aware of a recent, similar proposal to optically levitate and manipulate a nano-mechanical system by O. Romero-Isart et al., in arXiv:0909.1469.

1. Cleland A (2009) Optomechanics: Photons refrigerating phonons. *Nat Phys*, 5:458–460.
2. Genes C, Vitali D, Tombesi P (2008) Simultaneous cooling and entanglement of mechanical modes of a micromirror in an optical cavity. *New J Phys*, 10:095009.
3. Mamin HJ, Rugar D (2001) Sub-attonewton force detection at millikelvin temperatures. *Appl Phys Lett*, 79:3358–3360.
4. Maiwald R, et al. (2009) Stylus ion trap for enhanced access and sensing. *Nat Phys*, 5:551–554.
5. Cleland AN, Geller MR (2004) Superconducting qubit storage and entanglement with nanomechanical resonators. *Phys Rev Lett*, 93:070501.
6. Rabl P, et al. (2009) A quantum spin transducer based on nano electro-mechanical resonator arrays. *arXiv* 0908.0316.
7. Hao Z, Erbil A, Ayazi F (2003) An analytical model for support loss in micromachined beam resonators with in-plane flexural vibrations. *Sensor Actuat A-Phys*, 109:156–164.
8. Wilson-Rae I (2008) Intrinsic dissipation in nanomechanical resonators due to phonon tunneling. *Phys Rev B*, 77:245418.
9. Ashkin A (2007) *Optical Trapping and Manipulation of Neutral Particles Using Lasers: A Reprint Volume with Commentaires* (World Scientific, Singapore).
10. Ashkin A, Dziedzic JM (1976) Optical levitation in high vacuum. *Appl Phys Lett*, 28:333–335.
11. Libbrecht KG, Black ED (2004) Toward quantum-limited position measurements using optically levitated microspheres. *Phys Lett A*, 321:99–102.
12. Braginsky VB, Vyatchanin SP (2002) Low quantum noise tranquilizer for Fabry–Perot interferometer. *Phys Lett A*, 293:228–234.
13. Wilson-Rae I, Nooshi N, Zwerger W, Kippenberg TJ (2007) Theory of ground state cooling of a mechanical oscillator using dynamical backaction. *Phys Rev Lett*, 99:093901.
14. Marquardt F, Chen JP, Clerk AA, Girvin SM (2007) Quantum Theory of Cavity-Assisted Sideband Cooling of Mechanical Motion. *Phys Rev Lett*, 99:093902.
15. Zeng H, Lin F (1994) Quantum conversion between the cavity fields and the center-of-mass motion of ions in a quantized trap. *Phys Rev A*, 50:R3589–R3592.
16. Parkins AS, Kimble HJ (1999) Quantum state transfer between motion and light. *J Opt B-Quantum S O*, 1:496–504.
17. Zhang J, Peng K, Braunstein SL (2003) Quantum-state transfer from light to macroscopic oscillators. *Phys Rev A*, 68:013808.
18. Jähne K, et al. (2009) Cavity-assisted squeezing of a mechanical oscillator. *Phys Rev A*, 79:063819.
19. Takeno Y, Yukawa M, Yonezawa H, Furusawa A (2007) Observation of-9 dB quadrature squeezing with improvement of phase stability in homodyne measurement. *Opt Express*, 15:4321–4327.
20. Vahlbruch H, et al. (2008) Observation of squeezed light with 10-dB quantum-noise reduction. *Phys Rev Lett*, 100:033602.
21. Yonezawa H, Braunstein SL, Furusawa A (2007) Experimental demonstration of quantum teleportation of broadband squeezing. *Phys Rev Lett*, 99:110503.
22. Einstein A, Podolsky B, Rosen N (1935) Can quantum-mechanical description of physical reality be considered complete?. *Phys Rev*, 47:777–780.
23. McKeever J, et al. (2003) State-insensitive cooling and trapping of single atoms in an optical cavity. *Phys Rev Lett*, 90:133602.
24. Maunz P, et al. (2004) Cavity cooling of a single atom. *Nature*, 428:50–52.
25. Leibfried D, Blatt R, Monroe C, Wineland D (2003) Quantum dynamics of single trapped ions. *Rev Mod Phys*, 75:281–324.
26. Jost JD, et al. (2009) Entangled mechanical oscillators. *Nature*, 459:683–685.
27. Murch KW, Moore KL, Gupta S, Stamper-Kurn DM (2008) Observation of quantum-measurement backaction with an ultracold atomic gas. *Nat Phys*, 4:561–564.
28. Brennecke F, Ritter S, Donner T, Esslinger T (2008) Cavity Optomechanics with a Bose-Einstein Condensate. *Science*, 322:235–238.
29. Zener C (1932) Non-adiabatic crossing of energy levels. *P R Soc Lond A* 696–702.
30. Cirac JI, Zoller P, Kimble HJ, Mabuchi H (1997) Quantum state transfer and entanglement distribution among distant nodes in a quantum network. *Phys Rev Lett*, 78:3221–3224.
31. Beveratos A, Brouri R, Gacoin T, Poizat JP, Grangier P (2001) Nonclassical radiation from diamond nanocrystals. *Phys Rev A*, 64:061802.
32. Vernooy DW, Ilchenko VS, Mabuchi H, Streed EW, Kimble HJ (1998) High-Q measurements of fused-silica microspheresin the near infrared. *Opt Lett*, 23:247–249.
33. Bahns JT, Stwalley WC, Gould PL (1996) Laser cooling of molecules: A sequential scheme for rotation, translation, and vibration. *J Chem Phys*, 104:9689–9697.
34. Epstein PS (1924) On the resistance experienced by spheres in their motion through gases. *Phys Rev*, 23:710–733.
35. Hackermüller L, Hornberger K, Brezger B, Zeilinger A, Arndt M (2004) Decoherence of matter waves by thermal emission of radiation. *Nature*, 427:711–714.
36. Cirac JI, Blatt R, Zoller P, Phillips WD (1992) Laser cooling of trapped ions in a standing wave. *Phys Rev A*, 46:2668–2681.
37. Kokorowski DA, Cronin AD, Roberts TD, Pritchard DE (2001) From single-to multiple-photon decoherence in an atom interferometer. *Phys Rev Lett*, 86:2191–2195.
38. Hood CJ, Kimble HJ, Ye J (2001) Characterization of high-finesse mirrors: Loss, phase shifts, and mode structure in an optical cavity. *Phys Rev A*, 64:033804.
39. Pinard M, et al. (2005) Entangling movable mirrors in a double-cavity system. *Europhys Lett*, 72:747–753.
40. Gardiner CW, Collett MJ (1985) Input and output in damped quantum systems: Quantum stochastic differential equations and the master equation. *Phys Rev A*, 31:3761–3774.
41. Duan LM, Giedke G, Cirac JI, Zoller P (2000) Inseparability criterion for continuous variable systems. *Phys Rev Lett*, 84:2722–2725.
42. Julsgaard B, Kozhekin A, Polzik ES (2001) Experimental long-lived entanglement of two macroscopic objects. *Nature*, 413:400–403.
43. Rugar D, Grütter P (1991) Mechanical parametric amplification and thermomechanical noise squeezing. *Phys Rev Lett*, 67:699–702.
44. Gorodetsky ML, Pryamikov AD, Ilchenko VS (2000) Rayleigh scattering in high-Q microspheres. *J Opt Soc Am B*, 17:1051–1057.
45. Venkatathri N, Yoo JW (2008) Synthesis and characterization of silica nanosphere from octadecyltrimethoxy silane. *B Kor Chem Soc*, 29:29.
46. Shu J, et al. (2006) Elastic light scattering from nanoparticles by monochromatic vacuum-ultraviolet radiation. *J Chem Phys*, 124:034707.
47. Wineland DJ, et al. (2006) Trapped atomic ions and quantum information processing. *Proceedings of the International Conference on Atomic Physics (ICAP 2006)*, ed Roos C (Am Inst of Physics), pp 103–110.